



## Numerical study to optimize the efficiency of the OWC wave energy converter

Mamdouh Elmallah \*

*Department of Marine Engineering Technology, College of Maritime Transport & Technology, Arab Academy for Science, Technology, and Maritime Transport, Egypt.*

International Journal of Science and Research Archive, 2025, 14(03), 222-229

Publication history: Received on 29 January 2025; revised on 04 March 2025; accepted on 06 March 2025

Article DOI: <https://doi.org/10.30574/ijrsra.2025.14.3.0668>

### Abstract

Today, governments and researchers are keen on lowering thermal emissions caused by the combustion of fuel. Studies have demonstrated the risk of GHG emissions generated by traditional methods of energy generation, which contribute to global warming and climate change. This paper demonstrates the environmental effect of using the OWC wave energy converter to generate power. This numerical study investigates the effect of using a cylindrical air chamber to enhance the output power of the device. Modeling and numerical simulation are performed by using the commercial software ANSYS. The results show that the outlet air velocity increased from that of the conventional air chamber design to that of the cylindrical air chamber design by 42%. The air velocity in the cylindrical design reached 10.4 m/s.

**Keywords:** Ansys; Greenhouse Gases; Oscillating Water Column; Renewable Energy; Wave Energy

### 1. Introduction

Many researchers have confirmed that gasoline-oil is taken into consideration as the primary component that cause environmental and financial problems, particularly with the non-stop growing of gasoline cost (Elmallah et al., 2024; Elgohary & seddiek, 2013; Elmallah et al., 2024). Because of growing concerns about the environmental impact and cost of fossil fuels, research into alternative renewable energy sources has become increasingly critical (Elmallah et al., 2024; Elmallah, 2024). Wave energy conversion is one of renewable energy's most active study fields. Because of its simplicity, the oscillating water column (OWC) device is one of the most commonly used wave energy conversion methods (Elmallah et al., 2023). OWC provides numerous advantages because there are few moving parts. The OWC design is customizable. OWC may also be used on a variety of collector shapes along the coast, and the use of an air turbine avoids the need for gearboxes. OWC is dependable, easy to maintain, and makes efficient use of sea area.

\* Corresponding author: Mamdouh Elmallah

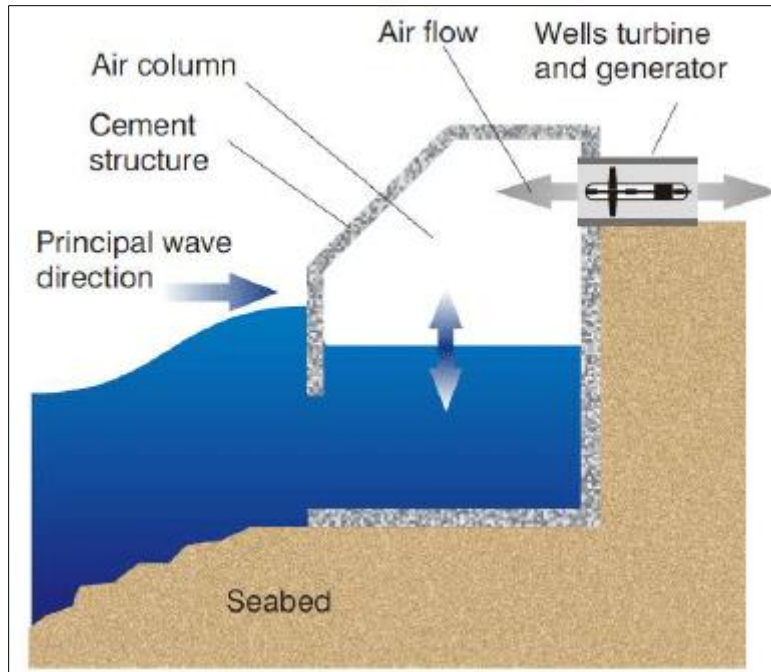


**Figure 1** Schematic layout of oscillating water column (OWC) system

As illustrated in Fig. 1, an OWC is made up of an empty chamber that is open to the sea under the surface, as well as an air turbine. The water column within the chamber oscillates due to wave action, compressing and decompressing the air in the upper half of the chamber alternately. The pressure difference between the interior of the chamber and the atmosphere allows air to flow in and out of the chamber, driving the turbine. Because of the flow's bidirectional nature, a novel approach is required to extract the greatest amount of available pneumatic energy per cycle. The most popular method is self-rectifying air turbines, which use a unidirectional rotation (Falcao, Henriques, Gato, 2018). The chamber geometry is just as critical as the turbine design when it comes to maximizing the performance of an OWC device. In the physical modelling studies, the impacts of the bottom slope and chamber width on response efficiency and energy absorption efficiency were investigated (Liu & Wu, 2002). To improve OWC wave energy device performance in a resonant state with the driving wave maintained, the tuning of an OWC seawater pump to polychromatic waves was examined (Godoy-Diana & Czitrom, 2007). A numerical model was utilized to forecast the flow characteristics of the components of an oscillating water column system used to capture wave energy (Marjani, Ruiz, Rodriguez, Santos, 2008). The power needed to compute OWC efficiency is calculated by integrating the product of air pressure in the chamber and airflow rate over time (Zhang, Zou, Deborah, 2012; Nunes, Valerio, Beirao, Costa, 2011; Sheng, Lewis, Alcorn, 2012). The hydraulic power can also be calculated by the simultaneous product of the displacement variation of the water-free surface and the chamber's air pressure, in this case, the water surface is represented as an oscillation flat plate (Stappenbelt & Cooper, 2010). In experimental work and in this study, the turbine was replaced with a circular hole (Sarmiento, 1992). The STAR-CCM+® was also used to describe the performance characteristics of single-chamber, dual-chamber, and fixed multi-chambers (Elhanafi et al., 2018; Shalby et al., 2019), as well as the hydrodynamic scale effects of an OWC (Dai et al., 2019). In the open-source Computational Fluid Dynamics (CFD) package REEF3D, Kamath et al. (Kamath, Bihs, Arntsen, 2015) investigated the effects of wavelength and steepness on the achievement of an OWC chamber and obtained a peak efficiency of 0.76. However, these studies focused only on the characteristics of the Oscillating Water Column and ignored chamber properties, despite its significant impact on the flow due to the continuity equations. The purpose of this paper is to simulate the wave system of OWC and to investigate the impact of using cylindrical air chamber design on air velocity entering the turbine using ANSYS FLUENT via Computational Fluid Dynamics (CFD), which is the proper approach to obtain the numerical solutions and deal with these complicated flow equations.

## 2. CFD simulation ANSYS-FLUENT

In the present study, a Volume of Fluid (VOF) model in ANSYS FLUENT, for the computational analysis of the OWC wave system, is established to study the air flow behaviour inside two different designs of air chambers. The air flow velocity is one of the most essential factors that affects the output power of the OWC device. The interface tracking between air and water phases is accomplished by the Volume of Fluid (VOF) method (Hirt & Nichols, 1981). The piecewise-linear

approach is used to calculate the interface between two fluids (Youngs, 1982). The FLUENT code is used to do flow simulations in order to determine the flow behaviour inside an OWC system's air chamber.

### 3. Model geometry and dimensions

The system proposed in this research is an example of an OWC wave energy conversion system. Figure 2 depicts the air chamber's key geometric features and model boundary definitions. The drawing depicts an air chamber with a hollow duct in the middle of its top. The hollow duct depicts the outlet airflow, which is intended to be the turbine inlet.

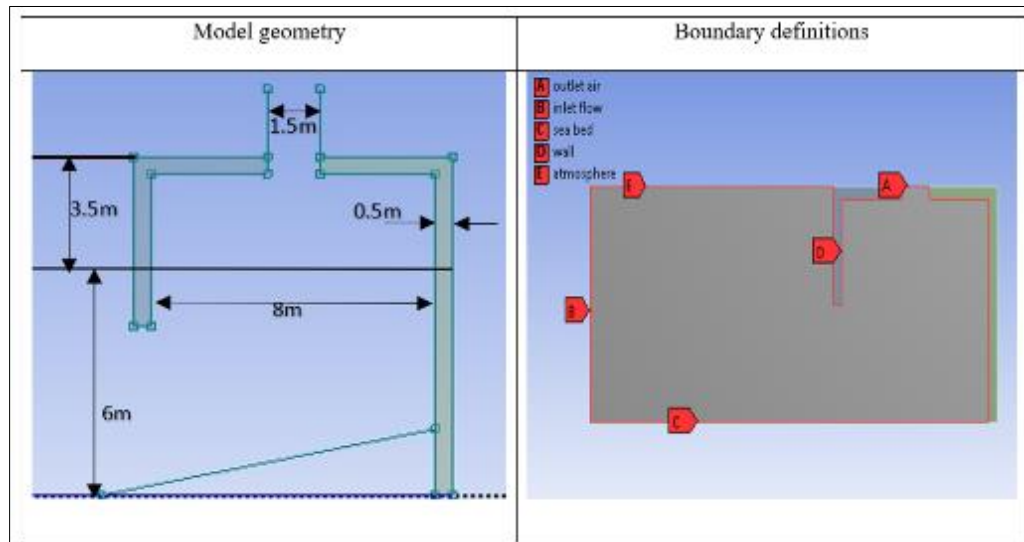


**Figure 2** The model geometry and boundary definitions

Figure 3 represents the two different cases of the air chamber designs that will be studied in this paper to show their impact on the outlet air velocity.

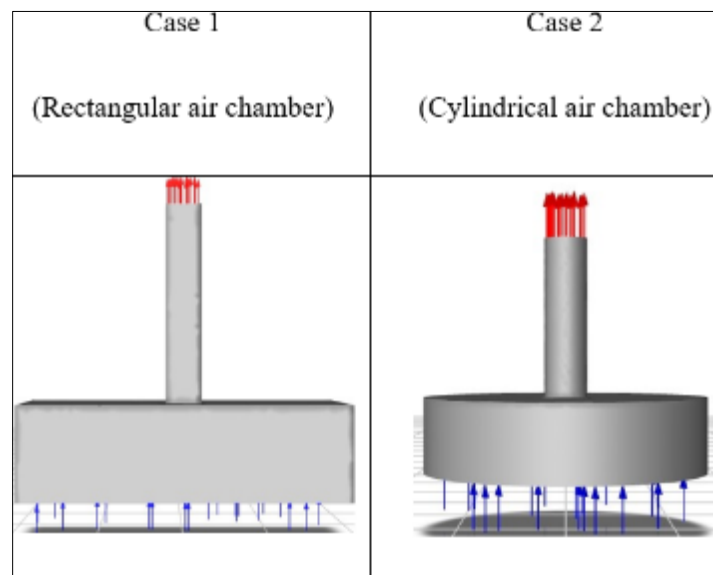


**Figure 3** the two different cases of the air chamber design

### 4. Generating mesh

A Finite Element Model (FEM) is a numerical approximation method that analyses the components of various structures by subdividing them into a small number of elements that connect with one another at points called nodes, and each

node may have two or more elements connected to it. A collection of these elements is known as a mesh. The creation of a grid of elements with which to solve the necessary fluid flow equations, as well as producing the high precision of the solution, makes model meshing the most crucial procedure in CFD simulation. Since reducing the element size has a substantial impact on computational time, in this mesh generation, the element size is 200 mm and the number of elements is 5956. The fine mesh of the model is shown in Fig.4.

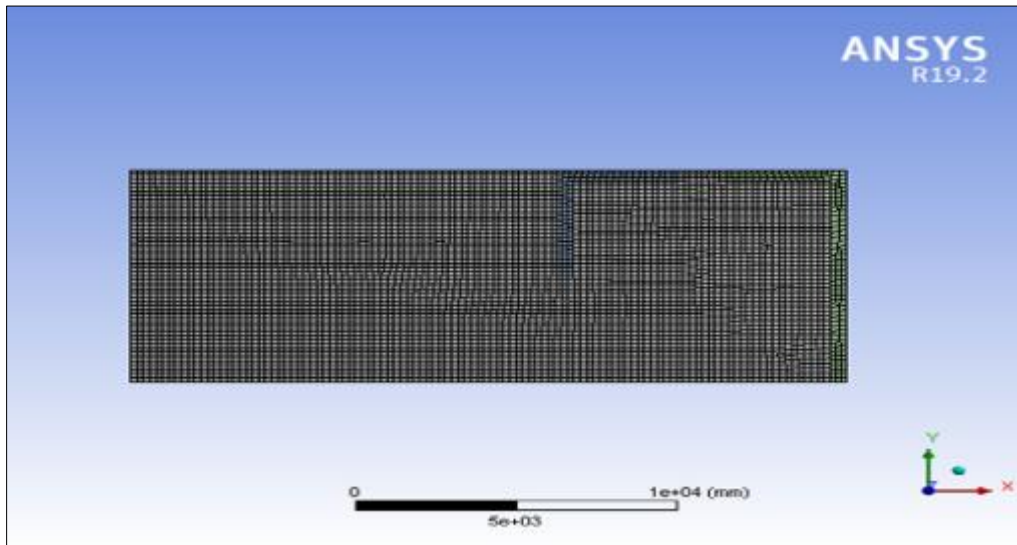


**Figure 4** fine mesh for the model

Figure 5 shows the generated mesh of the two different designs.

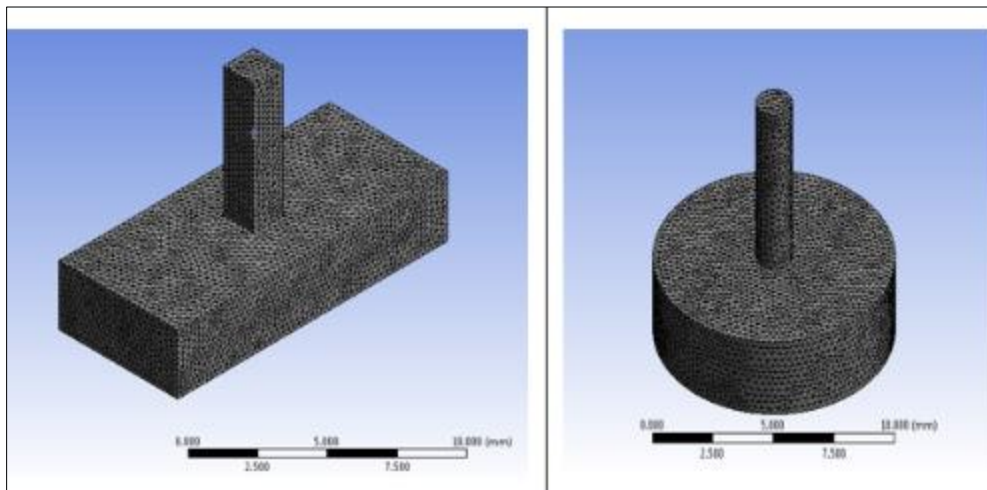


**Figure 5** the generated mesh of the two different designs

## 5. Solution setup

ANSYS FLUENT is selected to simulate the wave characteristics and to show the airflow behavior inside the air chamber. The linked conservation equations for mass, momentum, and energy are solved using the ANSYS FLUENT code. The classical k-model is used to simulate turbulent flow.

## 6. Governing equations

Fluid flow governing equations control mathematical operations and CFD calculations. These equations include the continuity equation, Reynolds Averaged Navier-Stokes (RANS) equations, and conservation equations of momentum and energy.

The following are the continuity equations and Reynolds Averaged Navier-Stokes (RANS) equations (Liu, Hyun, Hong, 2011):

$$\frac{\partial u_i}{\partial x_i} = 0 \quad \dots\dots\dots (1)$$

$$\frac{\partial \rho u_i}{\partial t} + \frac{\partial \rho u_i u_j}{\partial x_j} = -\frac{\partial p}{\partial x_i} + \rho f_{x_i} + \frac{\partial}{\partial x_j} \left( \nu \frac{\partial u_i}{\partial x_j} - \rho u'_i u'_j \right) \dots\dots\dots (2)$$

Where,  $\rho$ ,  $p$ , and  $f_{x_i}$  are the fluid density, fluid pressure, kinematic viscosity coefficient, and body force, respectively.  $x_i = (x, y, z)$  and  $u_i = (u, v, w)$  represent the Cartesian coordinates and corresponding Reynolds-averaged velocity components. The component  $\rho u'_i u'_j$  are called Reynolds stresses.

The following are the momentum and energy conservation equations [16]:

$$\frac{\partial \rho u}{\partial t} + \nabla \cdot (\rho u u) = -\nabla p + \nabla \cdot \tau + \rho g + F \dots\dots\dots (3)$$

$$\frac{\partial (\rho C_p T_f)}{\partial t} + \nabla \cdot (\rho C_p T_f u) = \nabla \cdot (\Psi_e \nabla T_f) + S_T \quad \dots\dots\dots (4)$$

where  $u$  is the fluid velocity vector;  $\tau$  is the viscous stress tensor;  $g$  is the gravitational acceleration;  $t$  is the time;  $F$  is the source of momentum due to surface tension;  $T_f$  is the temperature;  $C_p$  is the fluid specific heat;  $\Psi_e$  is the fluid thermal conductivity; and  $S_T$  is the source term in the energy equation.

The viscous stress tensor is:

$$\tau = \mu_{eff} [\nabla u + (\nabla u)^T] + \frac{2}{3} \mu_{eff} (\nabla \cdot u) I \quad \dots\dots\dots (5)$$

where  $I$  is the identity tensor and  $\mu_{eff}$  is the effective dynamic viscosity:

$$\mu_{eff} = \mu + \rho \nu_t \quad \dots\dots\dots (6)$$

where  $\mu$  is the dynamic viscosity of the fluid and  $\nu_t$  is the turbulent kinematic viscosity.

## 7. Turbulent model

To solve the given set of equations and explain the turbulence phenomena in the dynamic motions of water and air, the standard  $k$ - $\epsilon$  model, which is frequently used in engineering applications, must be applied, however some previous papers used  $k$ - $\omega$  model in their study for CFD simulation

## 8. Boundary conditions

All inlet and outlet parameters, in addition to the walls, are set during this phase. The wave theory is 5th-order-Stokes, Wave regime is Shallow/Intermediate, Wave Height ( $H$ ) is 1.3 m, Wave Length ( $L$ ) is 11.0 m, Liquid Depth ( $h$ ) is 6.0 m, and Ursell Number is 0.7282 m.

The following mandatory checks proved that the selected wave theory is appropriate for the simulation.

The relative Height:  $H/h = 0.2167$ , while Maximum theoretical limit = 0.7800 and Maximum numerical limit = 0.55.

The wave Steepness:  $H/L = 0.1182$ , while Maximum theoretical limit = 0.1420 and Maximum numerical limit = 0.1200

## 9. Validation and verification

According to experimental data derived from KORDI's physical modelling test (Hong et al., 2007), the CFD results validate, particularly for peak value prediction and amplitude ratios in the extended period domain. The peak value of air velocity for the rectangular air chamber reached 7.14 m/s and agrees with the experimental data.

## 10. Results and discussion

Since that this study is concerned about the effect of the air chamber design on the outlet air velocity flow, the wave simulation results of the outlet air velocity are applied as an inlet flow for each shape of the two cases. The results show that the outlet air velocity flow of the rectangular air chamber is 7.14 m/s, and the outlet air velocity flow of the cylindrical air chamber is 10.4 m/s. By applying the same air characteristics that were the result of the wave system simulation to two different air chamber designs, the results showed that the cylindrical shaped air chamber is the best shape that has the greatest outlet air velocity. Fig.6 shows the water volume fraction, the free surface, and different phases in the simulation.

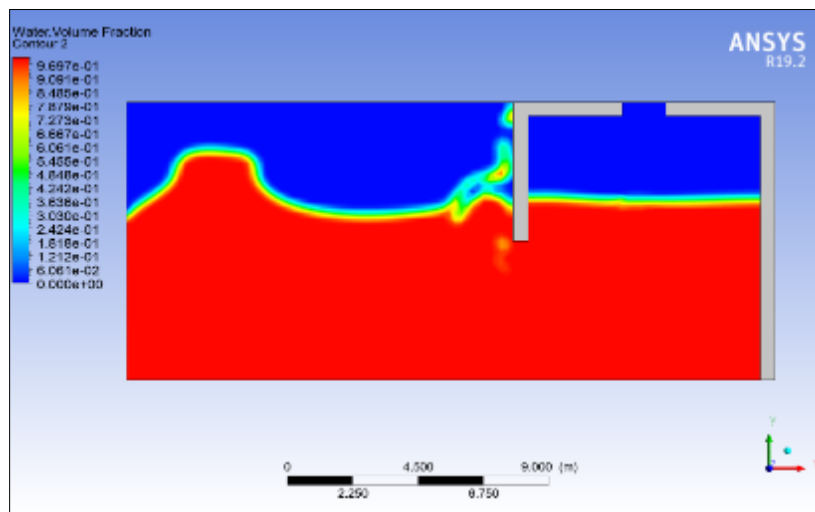


Figure 6 Water volume fraction contour

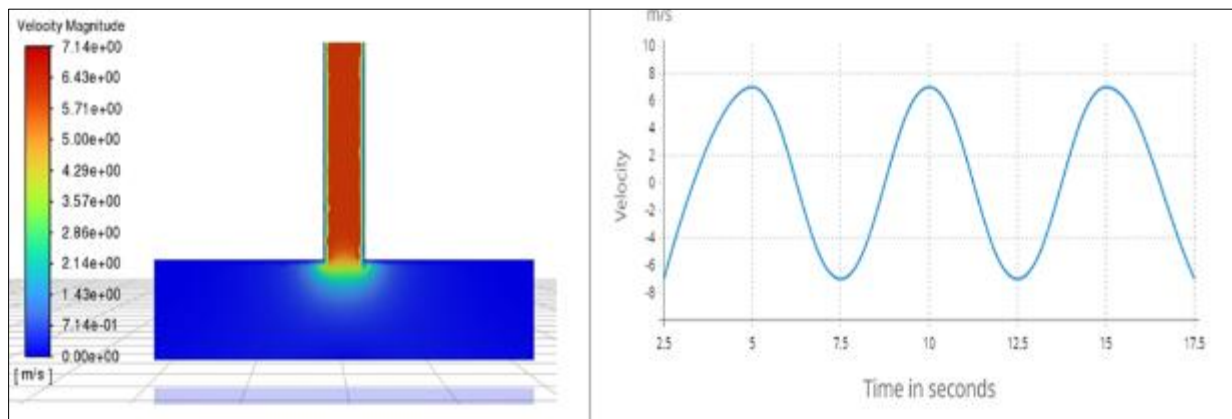
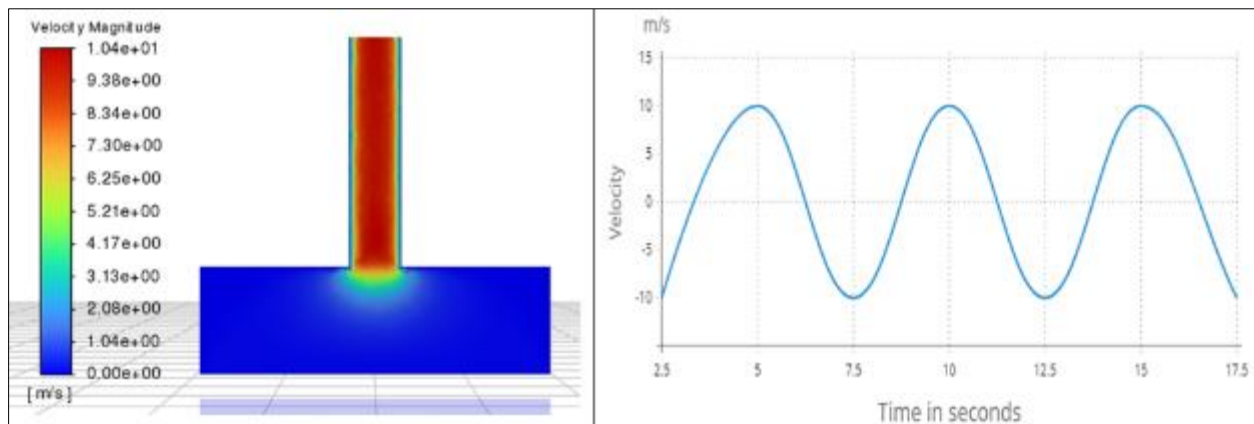


Figure 7 rectangular shaped air chamber

Although the CFD simulation calculates a vast amount of data, this study concerned only about the two cases outlet air velocity that will have a direct impact on the output power of the wave converter. In Case 1, Fig.7 show the outlet air



velocity contour and the time history of outlet air flow velocity in rectangular shaped air chamber. The velocity is 7.14 m/s for rectangular chamber. In Case 2, Fig.8 show the outlet air velocity contour and the time history of outlet air flow velocity in cylindrical shaped air chamber. the cylinder-shaped air chamber overcome the corner effects in rectangular shape and increase the velocity from 7.14 m/s into 10.14 m/s.



**Figure 8** Outlet air velocity of cylindrical shape air chamber

## 11. Conclusion

Burning fossil fuels is a major source of greenhouse gas emissions, which harm the environment and contribute to global warming and climate change. As a result, the globe has resorted to other petroleum sources for energy production. Renewable energy is one of the energy sources that the media is focusing on in order to eliminate the usage of fuel as a source of energy. This study focused on making adjustments to boost the efficiency of wave energy. The air velocity entering the turbine is one of the elements influencing the OWC's performance. The outlet air velocity flow is calculated using a simulated wave system with a VOF model in ANSYS FLUENT. In this study, the outlet air flow velocity of the wave system is studied separately while passing through two different air chamber designs. The results show that air chamber design significantly affects exit air velocity. Using a cylindrical shape reduces corner effects and improves air velocity to 10.14 m/s.

## References

- [1] Dai S, Day S, Yuan Z, Wang H. Investigation on the hydrodynamic scaling effect of an OWC type wave energy device using experiment and CFD simulation. *Renew Energy* 2019;142:184–94. <https://doi.org/10.1016/j.renene.2019.04.066>
- [2] El gohary, M. Morsy and Seddiek, I., (2013). Utilization of alternative marine fuels for gas turbine power plant onboard ship. *International Journal of Naval Architecture and Ocean Engineering*, 5(1), pp.141-149. <https://doi.org/10.2478/IJNAOE-2013-0115>
- [3] Elhanafi A, Macfarlane G, Ning D. Hydrodynamic performance of single-chamber and dual-chamber offshore-stationary Oscillating Water Column devices using CFD. *Appl Energy* 2018; 228:82–96. <https://doi.org/10.1016/j.apenergy.2018.06.069>
- [4] Elmallah, M. (2024, December 30). The impact of livestock emissions on the maritime sector. <https://www.jmr.unican.es/index.php/jmr/article/view/610>
- [5] Elmallah, M., Elgohary, M. M., & Shouman, M. R. (2023). The effect of air chamber geometrical design for enhancing the output power of oscillating water column wave energy converter. *Marine Technology Society Journal*, 57(1), 122–129. <https://doi.org/10.4031/mts.j.57.1.14>
- [6] Elmallah, M., Shouman, M., & Elgohary, M. (2024a, August 30). Numerical study on enhancing the performance of air turbines in Oscillating Water Column wave energy converters. <https://www.jmr.unican.es/index.php/jmr/article/view/1026>
- [7] Elmallah, M., Shouman, M., & Elgohary, M. (2024b). REDUCTION OF THE METHANE EMISSIONS ON LIVESTOCK SHIPS TO MITIGATE GREENHOUSE GAS EMISSIONS AND PROMOTE FUTURE MARITIME TRANSPORT SUSTAINABILITY. *Nativa*, 12(3), 551–558. <https://doi.org/10.31413/nat.v12i3.18180>

- [8] Elmallah, M., Shouman, M., & Elgohary, M. M. (2024). Reducing methane emissions on livestock ships in order to mitigate greenhouse gas emissions and promote future maritime sustainability. *TransNav the International Journal on Marine Navigation and Safety of Sea Transportation*, 18(4), 797–804. <https://doi.org/10.12716/1001.18.04.05>
- [9] Falcão, A. F. O., Henriques, J. C. C., & Gato, L. M. C., (2018). Self-rectifying air turbines for Wave Energy Conversion: A Comparative Analysis. *Renewable and Sustainable Energy Reviews*, 91, 1231–1241. <https://doi.org/10.1016/j.rser.2018.04.019>
- [10] Godoy-Diana, R. and Czitrom, S. P. R., (2007). On the tuning of a wave-energy driven oscillating-water-column sea water pump to polychromatic waves, *Ocean Eng.*, 34(17-18): 2374~2384. <https://doi.org/10.1016/j.oceaneng.2007.05.001>
- [11] Hirt, C. W. and Nichols, B. D., (1981). Volume of fluid (VOF) method for the dynamics of free, *Computational Physics*, 39(1): 201~225. [https://doi.org/10.1016/00219991\(81\)90145-5](https://doi.org/10.1016/00219991(81)90145-5)
- [12] Hong, K. Y., Shin, S. H., Hong, D. C., Choi, H. S. and Hong, S. W., 2007. Effects of shape parameters of OWC chamber in wave energy absorption, *Proc. 17th Int. Offshore and Polar Eng. Conf., Lisbon, Portugal, ISOPE*, 1, 428~433. <https://doi.org/10.1252/jcej.09we070>
- [13] Kamath A, Bihs H, Arntsen Ø A. Numerical investigations of the hydrodynamics of an oscillating water column device. *Ocean Eng* 2015;102:40–50. <https://doi.org/10.1016/j.oceaneng.2015.04.043>
- [15] Liu, Y. Q. and Wu, Q., (2002). Experimental investigation on the hydrodynamic performance of shoreline wave-power devices, *The Ocean Engineering*, 20(4): 93~97. <https://doi.org/10.1016/j.apenergy.2019.114252>
- [16] Liu, Z., Hyun, B. S., & Hong, K. (2011). Numerical study of air chamber for oscillating water column wave energy convertor. *China Ocean Engineering*, 25(1), 169–178. <https://doi.org/10.1007/s13344-011-0015-8>
- [17] López, I., Carballo, R., Fouz, D. M., & Iglesias, G., (2021). Design selection and geometry in owc wave energy converters for performance. *Energies*, 14(6). <https://doi.org/10.3390/en14061707>
- [18] Marjani, A. E., Ruiz, F. C., Rodriguez, M. A., & Santos, M. T. P., (2008). Numerical modeling in wave energy conversion systems, *Energy*, 33(8): 1246~1253. <https://doi.org/10.1016/j.energy.2008.02.018>
- [19] Nunes, G., Valério, D., Beirão, P., & Sá da Costa, J., (2011). Modelling and control of a wave energy converter. *Renewable Energy*, 36(7), 1913–1921. <https://doi.org/10.3182/20100329-3-PT-3006.00051>
- [20] Sarmento, A. J., (1992). Wave flume experiments on two-dimensional oscillating water column wave energy devices. *Experiments in Fluids*, 12(4-5), 286–292. <https://doi.org/10.1007/BF00187307>
- [21] Shalby M, Elhanafi A, Walker P, Dorrell DG. CFD modelling of a small scale fixed multi-chamber OWC device. *Appl Ocean Res* 2019;88:37–47. <https://doi.org/10.1016/j.apor.2019.04.003>
- [22] Sheng, W., Lewis, T., & Alcorn, R. (2012). On wave energy extraction of oscillating water column device, 4th International Conference on Ocean Energy. <https://doi.org/10.1016/j.apor.2012.05.004>
- [23] Stappenbelt, B. and Cooper, P., (2010). Mechanical Model of a Floating Oscillating Water Column Wave Energy Conversion Device. *Annual Bulletin of the Australian Institute of High Energetic Materials*, (1): 34-45. <https://doi.org/10.13140/2.1.1232.7688>
- [24] Youngs, D. L., (1982). Time-dependent multi-material flow with large fluid distortion, *Numerical Methods of Fluid Dynamics*, Academic Press, New York, 273-285.
- [25] Zhang, Y., Zou, Q. P., & Greaves, D. (2012). Air-water two-phase flow modelling of hydrodynamic performance of an oscillating water column device. *Renewable Energy*, 41, 159–170. <https://doi.org/10.1016/j.renene.2011.10.011>